0026-895X/97/061041-15$3.00/0

MOLECULAR PHARMACOLOGY, **52:**1041–1055 (1997).

Potent Inhibitors of Human Immunodeficiency Virus Type 1 Integrase: Identification of a Novel Four-Point Pharmacophore and Tetracyclines as Novel Inhibitors

NOURI NEAMATI, HUIXIAO HONG, SANJAY SUNDER, GEORGE W. A. MILNE, and YVES POMMIER

Laboratories of Molecular Pharmacology (N.N., S.S., Y.P.) and Medicinal Chemistry (H.H., G.W.A.M.), Division of Basic Sciences, National Cancer Institute, Bethesda, Maryland 20892

Received June 10, 1997; Accepted September 2, 1997

SUMMARY

A four-point pharmacophore was constructed from energy-minimized structures of chicoric acid and dicaffeoylquinic acid. The search of 206,876 structures in the National Cancer Institute 3D database yielded 179 compounds that contain this pharmacophore. Thirty-nine of these compounds were tested in an *in vitro* assay specific for human immunodeficiency virus type 1 integrase (IN). Each retrieved structure was fit to the pharmacophore, and the conformation that afforded the best fit was identified. Twenty of the 39 compounds tested exhibited IC_{50} values of <20 μM. Among the most potent inhibitors, tetracyclines emerged as a new class of inhibitors. Although the parent tetracycline exhibited marginal potency against purified IN, all substituted tetracyclines tested showed 5–100-fold increased potency. Disintegration assays with truncated IN mutants indicated that tetracyclines inhibit the IN catalytic core domain. To investigate whether chelation of divalent metals is implicated in differential potency of tetracyclines, enzyme assays were performed in the presence of both Mn^{2+} or Mg^{2+}; no significance difference in potency was observed. Rolitetracycline inhibited IN/DNA complex formation in the presence of EDTA, which suggests that inhibition was metal independent. Rolitetracycline reversed DNA binding of IN after the complex was allowed to form before the addition of drug. Selectivity of tetracyclines was also examined in an assay specific for topoisomerase I, and none of the tetracyclines tested induced topoisomerase I-mediated cleavable complex or inhibited camptothecin-induced cleavable complex. Remarkable potency against the IN in the absence of divalent metals and the core enzyme coupled with water solubility makes tetracyclines potential candidates for X-ray crystal structure determination with IN.

Several classes of inhibitors of HIV-1 IN have been reported (for recent reviews, see Refs. 1 and 2). Among these inhibitors, hydroxylated aromatics, which are present in a variety of natural products, have consistently exhibited remarkable potency in *in vitro* assays specific for IN. Although they are from a variety of unrelated families, the majority of these inhibitors share a common structural feature of two aryl units separated by a central linker (examples are shown in Fig. 1). The recurring requirement of a catechol moiety is a common theme among hydroxylated aromatic inhibitors of IN. Catechols, however, do not have desirable properties in the cell-based assay against HIV-1 infection; many of them retain high cytotoxicity. Oxidation of catechol units *in situ* to quinones may contribute to their cytotoxicity. Recent reports by Robinson *et al.* (3, 4) indicate that the caffeoylquinic acids and chicoric acid, both of which contain two catechol moieties, exhibit remarkable antiviral activity with high potency against IN.

Several other studies on the antiviral activity and cytotoxicity of chicoric acids have appeared since the isolation and synthesis of the parent compound were first reported by Scarpati and Oriente (5). For example, chicoric acid and caffeic acid reduced infectivity of vesicular stomatitis virus in mouse L-929 cells only after infection with vesicular stomatitis virus (6). These compounds provide no prophylactic properties; no antiviral effects were observed when L-929 cells were treated before vesicular stomatitis virus infection (6). A variety of polyhydroxylated carboxylic acids have been reported to inhibit HIV-1 replication, perhaps through interaction with gp120 and prevention of virus binding to the CD_4 receptor. For example, Mahmood *et al.* (7) reported that 4,5-di-*O*-caffeoylquinic acid interacts irreversibly with gp120. Moreover, galloylquinic acids were reported to possess biological activities that included inhibition of HIV-1 reverse transcriptase and human DNA polymerases α, β, and γ (8).

Other biological properties of plant polyphenols include anticarcinogenic, anti-inflammatory, antibacterial, immune-stimulating, antiallergic, and ostrogenic effects and inhibi-

ABBREVIATIONS: HIV-1, human immunodeficiency virus type 1; IN, integrase; RMS, root-mean-square; DCQA, dicaffeoylquinic acid; 1-MO-3,5-DCQA, 1-methoxyoxalyl-3,5-dicaffeoylquinic acid; HPLC, high performance liquid chromatography; DMSO, dimethylsulfoxide; NDGA, nordihydroguaiaretic acid; SDS, sodium dodecyl sulfate; HEPES, 4-(2-hydroxyethyl)-1-piperazineethanesulfonic acid; 3D, three-dimensional.

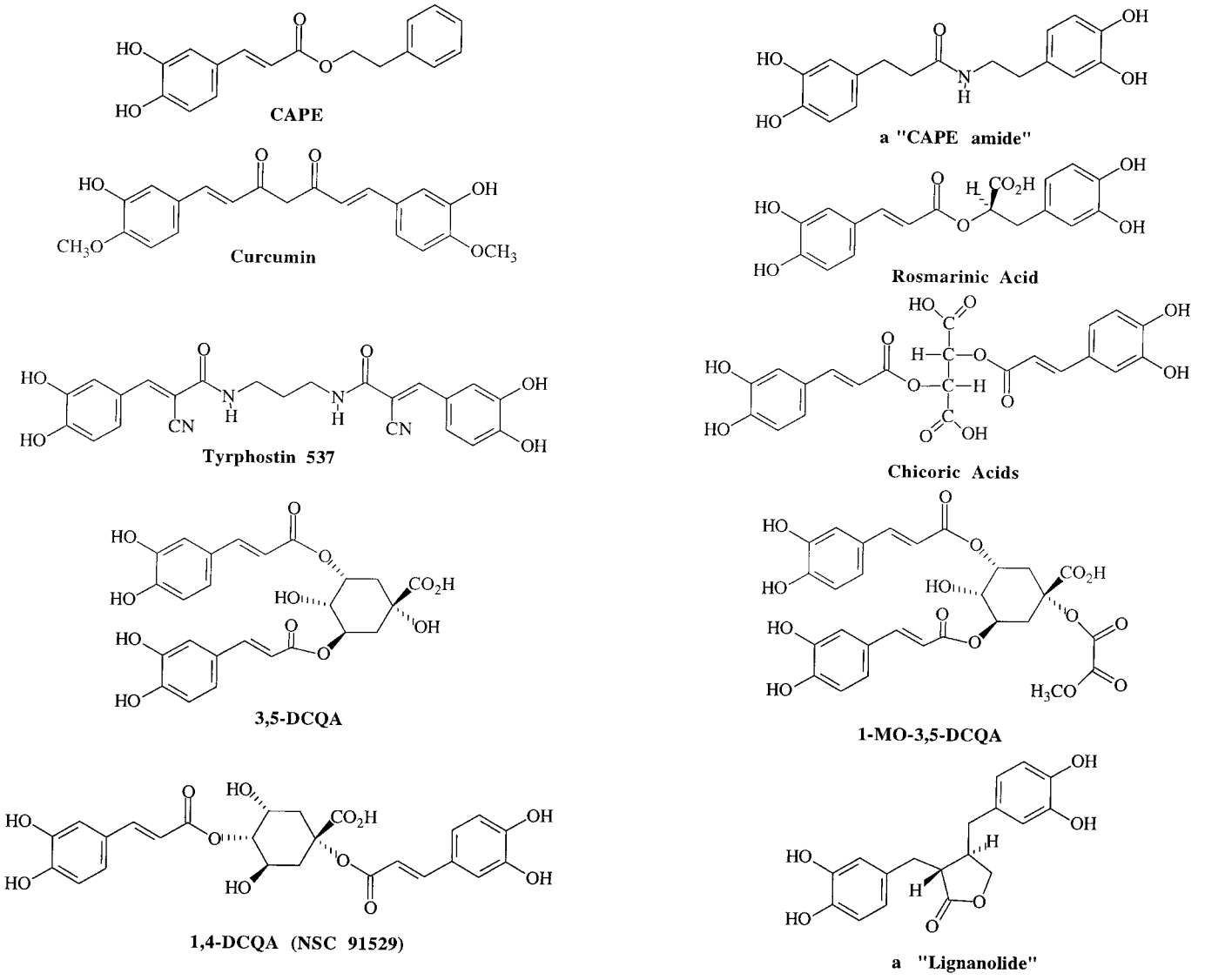

Fig. 1. Structures of several known hydroxylated aromatic inhibitors of HIV-1 integrase. *CAPE*, caffeic acid phenethyl ester.

tion of cyclo-oxygenase, lipoxygenase, and phospholipase A (9). Plant polyphenols are in general multifunctional and can act as reducing agents, hydrogen-donating antioxidants, metal chelators, and singlet-oxygen quenchers (9).

In our search for novel IN inhibitors, we have identified many hydroxylated aromatic inhibitors of IN (1, 2). Although they are in general cytotoxic or inactive against HIV-1 replication in cell-based assays, their use as lead compounds for the design of noncatechol-containing inhibitors has been indispensable, and their contribution to our structure-activity studies has helped to elucidate the structural requirement for cytotoxicity and activity. We previously identified a series of novel inhibitors of IN based on three-point pharmacophores that were used in searches of the National Cancer Institute 3D database to identify numerous IN inhibitors (10–12). Evidence was obtained that suggested that some of these three-point pharmacophores were in fact part of a four-point pharmacophore; we have now extended those studies to characterize such a pharmacophore. This pharmacophore has been built from the low energy conformations of chicoric acid and caffeoylquinic acids, and its use in a search of the National Cancer Institute 3D database yielded several novel inhibitors; among them, a series of tetracyclines were identified as potent inhibitors and studied further to characterize their molecular interaction with IN.

Experimental Procedures

Chemicals. Tetracycline, oxytetracycline, doxycycline, methacycline, and rolitetracycline were obtained from Sigma Chemical (St. Louis, MO). All of the other compounds used in this study were obtained from the National Cancer Institute chemical repository through the Drug Synthesis and Chemistry Branch (Bethesda, MD). All compounds were dissolved in DMSO, and the stock solutions were stored at −20°.

Preparation of oligonucleotide substrates. The high performance liquid chromatography-purified oligonucleotides AE117, 5′-ACTGCTAGAGATTTTCCACAC-3′; AE118, 5′-GTGTGGAAAATCTCTAGCAGT-3′; AE157, 5′-GAAAGCGACCGCGCC-3′; AE146, 5′-GGACGCCATAGCCCCGGCGCGGTCGCTTTC-3′; AE156, 5′-GTGTGGAAAATCTCTAGCAGGGGCTATGGCGTCC-3′; RM22M, 5′-TACTGCTAGAGATTTTCCACAC-3′; and RMAB2, 5′-GTGTGGAAAATCTCTAGCUGT-3′ were purchased from Midland Certified Re-

agent Company (Midland, TX). Purified recombinant IN deletion mutant IN^{50-212}, expression system for the wild-type IN and the IN^{50-212} (F185K), were generous gifts of Drs. T. Jenkins and R. Craigie (Laboratory of Molecular Biology, National Institute of Diabetes and Digestive and Kidney Diseases, National Institutes of Health, Bethesda, MD). To analyze the extents of 3′-processing and strand transfer using 5′-end-labeled substrates, AE118 was 5′-end labeled using T_4 polynucleotide kinase (GIBCO BRL, Gaithersburg, MD) and [γ-^{32}P]ATP (DuPont-New England Nuclear, Boston, MA). To determine the extent of 30-mer target strand generation during disintegration, AE157 was 5′-end labeled and annealed to AE156, AE146, and AE117. The kinase was heat inactivated, and AE117 was added to the same final concentration. The mixture was heated at 95°, allowed to cool slowly to room temperature, and run through a G-25 Sephadex quick-spin column (Boehringer-Mannheim Biochemicals, Indianapolis, IN) to separate annealed double-stranded oligonucleotide from unincorporated label.

To analyze the extent of site-specific cleavage of 3′-end-labeled substrate by IN, AE118 was 3′-end labeled using [α-^{32}P]cordycepin triphosphate (DuPont-New England Nuclear) and terminal transferase (Boehringer-Mannheim Biochemicals). The transferase was heat inactivated, and RM22M was added to the same final concentration. The mixture was heated at 95°, allowed to cool slowly to room temperature, and analyzed on a G-25 Sephadex quick-spin column as before.

To determine the extent of Schiff base formation (13), RMAB2 was 5′-end labeled and allowed to react with AE117 as described above. The uracil was removed from duplex oligonucleotides that contained deoxyuridine by incubation of 40 μl of end-labeled DNA (500 nM stock solution) with 1 unit of uracil DNA glycosylase (Life Technologies, Grand Island, NY) for 90 min at 30°. The reaction was then loaded onto a G-25 Sephadex quick-spin column to remove the unincorporated label and the uracil.

IN assays. To determine the extent of 3′-processing and strand transfer, IN was preincubated at a final concentration of 200 nM with the inhibitor in reaction buffer [containing 50 mM NaCl, 1 mM HEPES, pH 7.5, 50 μM EDTA, 50 μM dithiothreitol, 10% glycerol (w/v), 7.5 mM $MnCl_2$, 0.1 mg/ml bovine serum albumin, 10 mM 2-mercaptoethanol, 10% DMSO, and 25 mM 3-(*N*-morpholino)propanesulfonic acid, pH 7.2] at 30° for 30 min (14). Then, 20 nM of the 5′-end ^{32}P-labeled linear oligonucleotide substrate was added, and incubation was continued for an additional hour. Reactions were quenched by the addition of an equal volume (16 μl) of loading dye (98% deionized formamide, 10 mM EDTA, 0.025% xylene cyanol, 0.025% bromphenol blue). An aliquot (5 μl) was electrophoresed on a denaturing 20% polyacrylamide gel (0.09 M Tris-borate, pH 8.3, 2 mM EDTA, 20% acrylamide, 8 M urea).

Gels were dried, exposed in a Molecular Dynamics (Sunnyvale, CA) PhosphorImager cassette, and analyzed using a Molecular Dynamics PhosphorImager. Percent inhibition was calculated using the following equation: $I\,(\%) = 100 \times [1 - (D - C)/(N - C)]$, where C, N, and D are the fractions of 21-mer substrate converted to 19-mer (3′-processing product) or strand transfer products for DNA alone, DNA plus IN, and IN plus drug, respectively. All IC_{50} values were determined by plotting the drug concentration versus percent inhibition and determining the concentration that produced 50% inhibition.

To determine the effects of drugs on the choice of nucleophile in the 3′-processing, reactions were performed essentially as described above with a 3′-end-labeled oligonucleotide (15). Disintegration reactions were performed as above with a Y oligonucleotide (i.e., the branched substrate in which the U5 end was "integrated" into target DNA) (16).

DNA binding assay using Schiff base formation. This assay was described in detail recently (13). Briefly, IN (200 nM) was preincubated with the inhibitor (at the indicated concentration) for 30 min at 30°. Subsequently, an oligonucleotide that contained an abasic site (13) (see Fig. 9A) in reaction buffer (described above) was added for 2 min at room temperature. A freshly prepared solution of sodium borohydride (0.1 M final concentration) was added, and reaction was continued for an additional 2 min. An equal volume (16 μl) of 2× SDS-polyacrylamide gel electrophoresis buffer (100 mM Tris, pH 6.8, 4% 2-mercaptoethanol, 4% SDS, 0.2% bromphenol blue, 20% glycerol) was added to each reaction, and the reaction was heated at 95° for 3 min before loading a 20-μl aliquot onto a 12% SDS-polyacrylamide gel. The gel was run at 120 V for 1.5 hr, dried, and exposed in a PhosphorImager cassette. Gels were analyzed using a Molecular Dynamics PhosphorImager.

Topoisomerase reactions. Reactions were performed in 10 μl of reaction buffer (0.01 M Tris·HCl, pH 7.5, 150 mM KCl, 5 mM $MgCl_2$, 0.1 mM EDTA, 15 mg/ml bovine serum albumin) with the following duplex oligonucleotide substrate (17) labeled with α-^{32}P-cordycepin at the 3′-end of the upper strand (*): 5′-GATCTAAAAGACTT GGAAAA-ATTTTTAAAAAA*ATTTTCTGAA-CCTTTTTAAAAATTTTTTCTAG-5′. This oligonucleotide contains a single topoisomerase I cleavage site (caret in upper strand). Approximately 50 fmol of oligonucleotide/reaction was incubated with 10 units of calf thymus DNA topoisomerase I (GIBCO BRL). Reactions were stopped by the addition of SDS (0.5% final concentration). Proteolysis was halted by the addition of 36 μl of 2.5× loading buffer (98% formamide, 0.01 M EDTA, 1 mg/ml xylene cyanol, 1 mg/ml bromphenol blue). An aliquot (5 μl) was electrophoresed on a denaturing 20% polyacrylamide gel (0.09 M Tris-borate, pH 8.3, 2 mM EDTA, 20% acrylamide, 8 M urea).

National Cancer Institute 3D database and search software. The National Cancer Institute 3D database and the Chem-X program used in both 3D database build and search processes have been described previously (18–20). The current version of the National Cancer Institute 3D database consists of 206,876 open and 201,036 discrete (proprietary) structures, for a total of 407,912 structures. All searches reported in this article were conducted only within the open part of the database. The conformational flexible search algorithm implemented in Chem-X (July 1994 version; Chemical Design, Oxford, UK) running on a Silicon Graphics IRIS Indigo workstation (Mountain View, CA) was used. For flexible compounds, multiple conformations are generated and analyzed during both building and searching of the database. A pharmacophore in this study refers to the 3D arrangement of those atoms in a compound that is responsible for the biological activity of the compound. Three-dimensional database pharmacophore searching facilitates identification of molecules that meet the requirements specified in the pharmacophore query. This approach has gained attention recently for its use in the discovery of new leads in drug development programs, and we have built a searchable 3D database (18) with a total of ≈407,000 structures from the two-dimensional structures of the National Cancer Institute Drug Information System database (19) using the program Chem-X. Use of 3D database searching has enabled us to identify a number of novel protein kinase C agonists (21), as well as HIV-1 protease (22) and IN inhibitors (10–12).

Molecular modeling. All molecular modeling studies were performed with the QUANTA 4.0/CHARMm 22 (Molecular Simulations, Burlington, MA) molecular modeling package running on a Silicon Graphics IRIS Indigo workstation. Energy minimization was typically computed with 5000 iterations or until convergence (defined as an energy gradient of ≤0.001 Kcal/mol/Å), using an Adjusted Basis Newton-Raphson algorithm as implemented in CHARMm. The structures of compounds were built using the ChemNote module with QUANTA and were energy-minimized using CHARMm. Conformational searches were conducted using the Monte Carlo random search algorithm implemented in QUANTA.

Results and Discussion

Identification of a unique four-point pharmacophore. Recently, we reported the identification of two distinct three-point pharmacophores among a series of lichen acids

(10). Searches of the National Cancer Institute 3D database with these pharmacophores yielded ≈800 compounds that contained either of these pharmacophores; the dicaffeoylquinic acids were identified in this way as potent inhibitors of IN. Robinson *et al.* (3, 4) reported anti-HIV-1 activity for the caffeoylquinic class of compounds. To determine the biologically active conformation of 1-MO-3,5-DCQA, 3,5-DCQA, and L-chicoric acid, 5000 conformations were generated in each case with the use of a random sample generator in QUANTA. Each of the conformations was minimized with the Adjusted Basis Newton-Raphson algorithm in CHARMm (23) using 5000 iterations or until convergence defined as an energy gradient of 0.001 Kcal/mol/Å. The unique four-point pharmacophore was identified in each case from analysis of the low energy ($\Delta E < 4.7$ Kcal/mol) conformations of these three compounds. The pharmacophore query shown in Fig. 2 was built from the 3D structures of 1-MO-3,5-DCQA, 3,5-DCQA, and L-chicoric acid, whose structures are shown in Fig. 1. These compounds possess the three-point pharmacophores defined previously (10–12); it was envisaged that four-point pharmacophores should be both more precise and more specific. Compounds that contained a four-point pharmacophore should bind more effectively than those with only a three-point pharmacophore. The pattern of six distances in a four-point pharmacophore is more stringent than that of the three distances in a three-point pharmacophore, and fewer hits should be expected in a search. Molecular modeling studies of 1-MO-3,5-DCQA, 3,5-DCQA, and L-chicoric acid enabled us to identify the novel four-point pharmacophore shown in Fig. 2. These three IN inhibitors fit this four-point pharmacophore in low energy conformations (ΔE = 1.25, 4.37, and 4.67 Kcal/mol, respectively), and the superimposition on one another of the four-point pharmacophores in the best-fit conformations of these inhibitors, a view of which is shown in Fig. 3, gave RMS values of 0.334, 0.209, and 0.055Å. From this four-point pharmacophore, we can generate four independent three-point pharmacophores with distance patterns: 9.5, 8.6, and 2.6 Å; 11.5, 9.5, and 2.6 Å; 10.5, 8.6, and 2.6 Å; and 11.5, 10.5, and 2.6 Å.

The first of these, the three-point pharmacophore with distance pattern of 9.5, 8.6, and 2.6 Å, is close to the three-point pharmacophores described previously (10–12), which

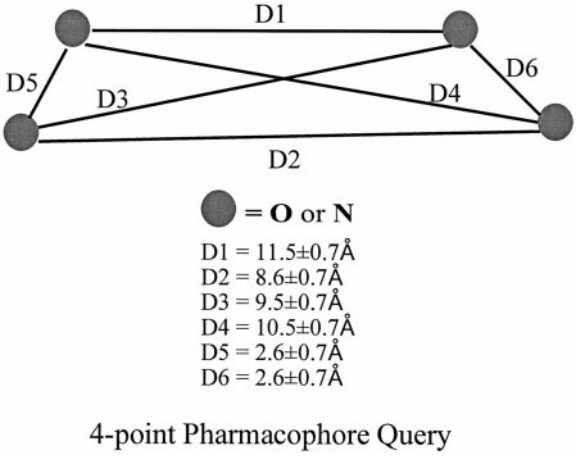

Fig. 2. Dimensions of four-point pharmacophore queries. In searching the National Cancer Institute 3D database, a basic nitrogen atom was allowed in place of oxygen.

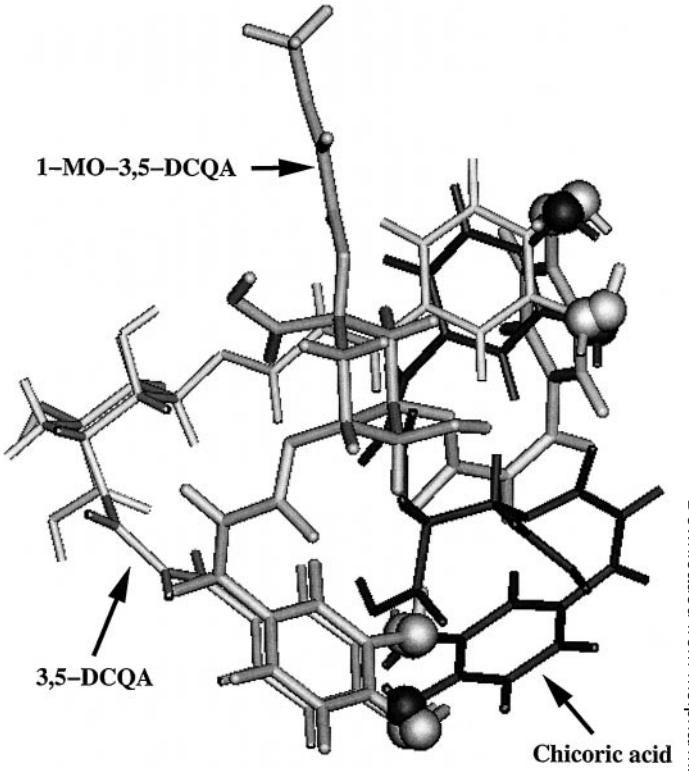

Fig. 3. Four-point pharmacophore superimposition (RMS = 0.334, 0.209, and 0.055 Å) of chicoric acid (*dark gray lines*), 3,4-DCQA acid (*light gray lines*), and 3,5-DCQA (*thick lines*).

have the dimensions 8.01, 2.71, and 8.73 Å and 8.71, 2.55, and 9.05 Å.

To adopt the conformation that contains the pharmacophore and is required for binding to its target, a compound may have some conformational energy penalty, but this energy penalty cannot exceed the overall binding free energy gained through the binding process. The biologically active conformation of an inhibitor need not be its global energy minimum, but it must be a low energy conformation.

3D database search. The four-point pharmacophore was used in a search of the National Cancer Institute 3D database. The distance tolerances in the pharmacophore query were set to 0.7 Å, as shown in Fig. 2. Every atom in the pharmacophore was allowed to be either oxygen or an amino nitrogen. The 3D database search of 206,876 structures yielded a total of 179 compounds that contain this four-point pharmacophore distance pattern in one or more of their conformations. Thirty-nine compounds (Fig. 4) were manually selected for bioassay based on considerations of structural diversity and sample availability, with the most probable four-point pharmacophore centers identified. It is important to note that several of the compounds selected by the four-point pharmacophore presented in this study would also fit the previously described three-point pharmacophore. However, the three-point pharmacophore in general yielded a higher number of hits. On the other hand, the four-point pharmacophore yielded a greater number of active inhibitors (see below).

Influence of conformational energy penalty and geometric fitness. All 39 compounds were initially tested in the IN assay at 100 μg/ml (Table 1). Compounds with inhibitory potency >50% were further assayed at different concentra-

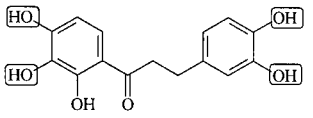

(1) NSC 309121

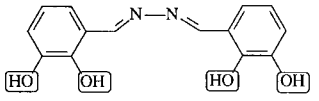

(2) NSC 318213

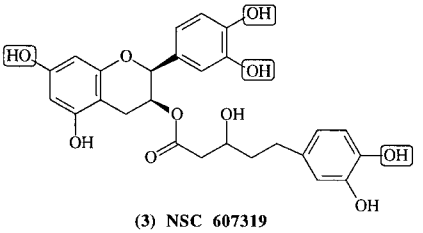

(3) NSC 607319

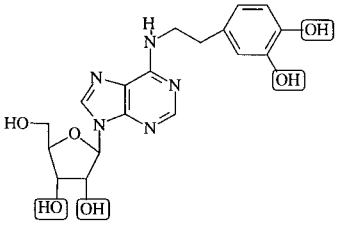

(4) NSC 281311

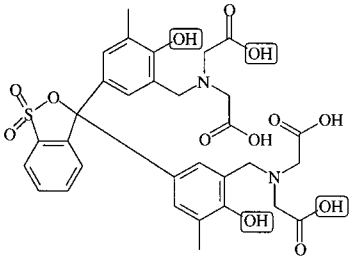

(5) NSC 324982

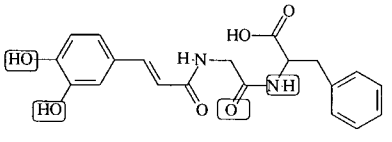

(6) NSC 332542

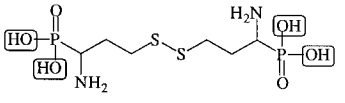

(7) NSC 359095

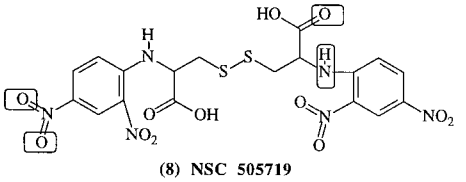

(8) NSC 505719

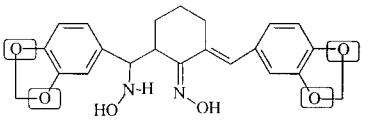

(9) NSC 632823

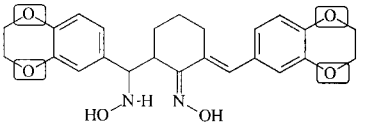

(10) NSC 636681

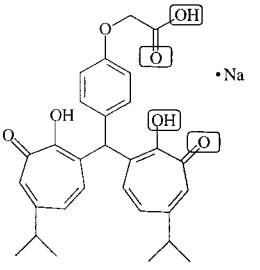

(11) NSC 624404

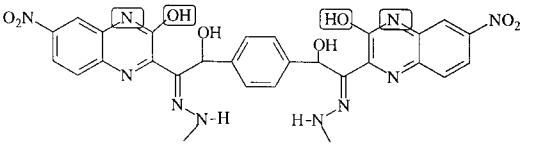

(12) NSC 642651

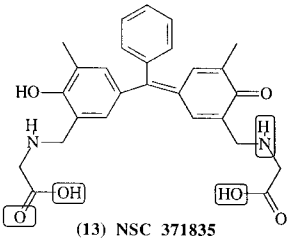

(13) NSC 371835

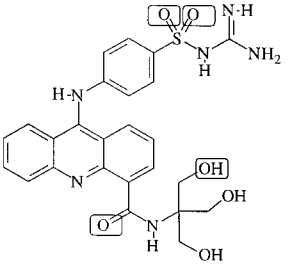

(14) NSC 674503

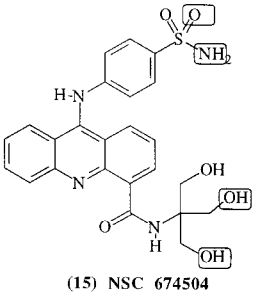

(15) NSC 674504

Fig. 4. Structures of compounds that contain the four-point pharmacophore.

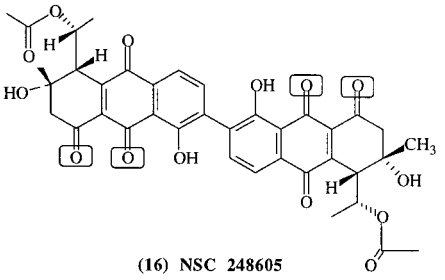

(16) NSC 248605

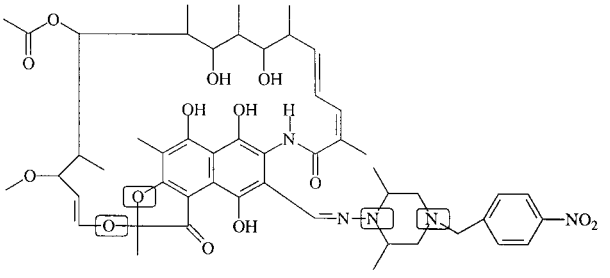

(21) NSC 233026

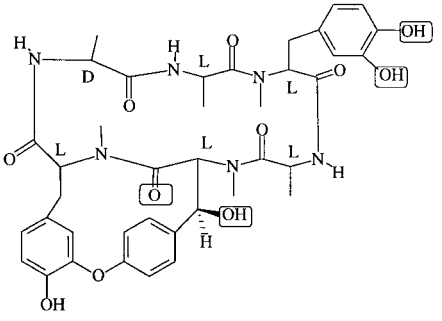

(17) NSC 328421

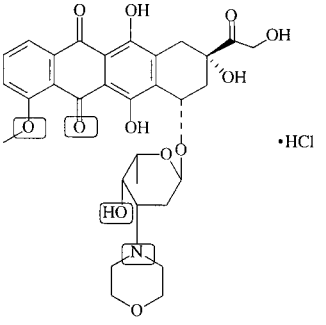

(22) NSC 354646

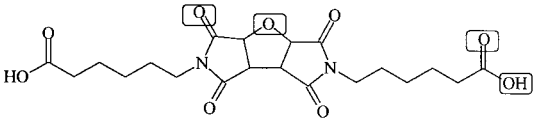

(18) NSC 192709

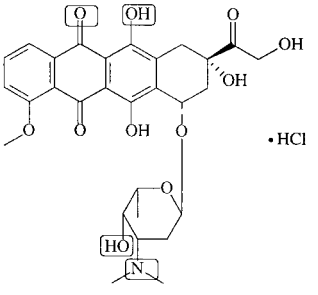

(23) NSC 261045

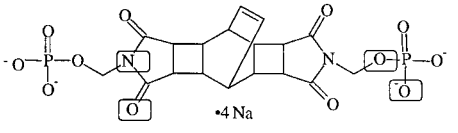

(19) NSC 600267

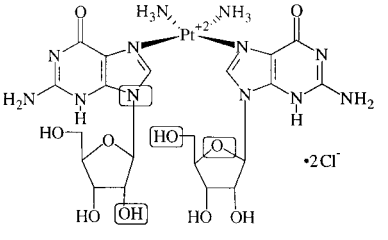

(24) NSC 267583

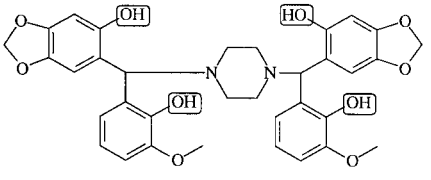

(20) NSC 369085

Fig. 4.—(*Continued*)

tions to determine their IC_{50} values. Twenty (51%) exhibited IC_{50} values of <20 μM and 24 (62%) exhibited IC_{50} values at <100 μM (Table 1), which suggests that the pharmacophore query used for searching is effective in identifying active compounds. However, 15 of the compounds were inactive ($IC_{50} > 100$ μM), so the four-point pharmacophore query defined in Fig. 2 seems to be necessary but not sufficient to determine effective binding of the ligand to IN. Other factors such as hydrophobicity and molecular shape effects could be responsible for the biological inactivity of compounds that contain the pharmacophore. Two factors that contribute to the structure-activity relationships are the conformational energy penalty and the geometric fitness of the pharmacophore in the ligand binding conformation. The larger the conformational energy penalty, the more difficult it will be for the inhibitor to adopt the desired conformation and less precise its binding will be to the enzyme. The better the enzyme-ligand fit, the more potent is the inhibitor.

The conformational energy penalty problem is a caveat in the Chem-X search software. The 3D database pharmacoph-

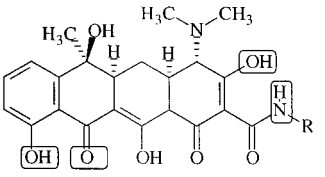

Compound	R	Compound	R
(25) Tetracycline	H	(33) NSC 69318	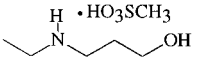
(26) Rolitetracycline	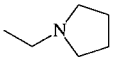	(34) NSC 64452	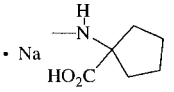
(27) NSC 43891	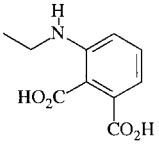	(35) NSC 67586	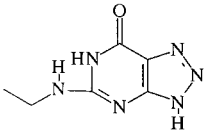
(28) NSC 43889	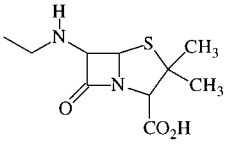	(36) NSC 69319	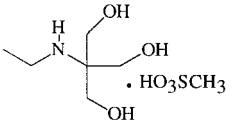
(29) NSC 56714	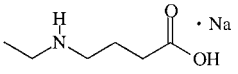	(37) NSC 69326	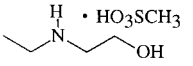
(30) NSC 56712	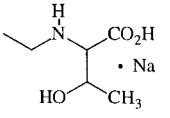	(38) NSC 69345	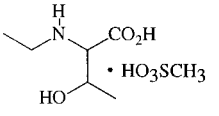
(31) NSC 64205	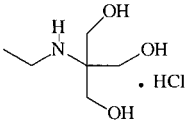	(39) NSC 118695	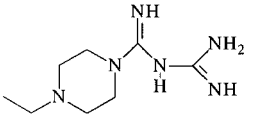
(32) NSC 64431	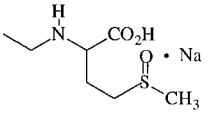		

Fig. 4.—(*Continued*)

ore search does not explicitly take into account the energy of each conformation, and consequently, some structures found by Chem-X had little or no inhibitory activity because only a high energy conformation fit the pharmacophore query. To investigate the influence of this conformational energy penalty on the binding of inhibitors to IN, pharmacophore mapping was carried out for all of the 39 compounds. Four thousand conformations of each structure were randomly generated and minimized with 5000 iterations or until convergence. These conformations were then mapped onto the pharmacophore query constructed in Fig. 2, and the results are shown in Table 1.

The RMS values of the conformations mapped onto the four-point pharmacophore query are given in Table 1 and are estimates of the geometric fitness of the four-point pharmacophore in the binding conformation. The difference in energy (ΔE) between this conformation and the global minimum is also given. The conformational energy penalty and RMS value should both influence the potency of an inhibitor; these two factors are represented in the following equation: $F = (\Delta E_1 - \Delta E_2)(RMS)$, where F represents the relation between inhibitor activity and the conformational energy penalty and geometric fit. The ΔE_1 refers to the energy difference between the lowest energy conformer and the superimposition conformer of the indicated compounds onto the four-point pharmacophore. The ΔE_2 represents a hypothetical energy penalty related to the conformational change and is derived from the analysis of small molecule/protein complexes; this value is assigned as -7 Kcal/mol (24) in the above equation. RMS refers to RMS of superimposition of the indicated compound onto a four-point pharmacophore. This arbitrary equation provides the plot shown in Fig. 5, in which it can be seen that small F values denote a better geometric fit (i.e., smaller RMS) and/or a low conformational energy penalty, both of which are compatible with increased potency of the inhibitor. Fig. 5 shows that this device serves to distinguish the 24 active compounds ($IC_{50} < 100\ \mu M$) from the 15 less active compounds and provides qualitative support

TABLE 1

Correlation between anti-HIV-1 integrase activities of a series of four-point pharmacophore containing drugs with their corresponding RMS and ΔE_1 values

Purified recombinant HIV-1 integrase was treated with different concentrations of drugs as described in Experimental Procedures to obtain IC_{50} values. RMS values refer to root-mean-square of superimposition of indicated compound onto the four-point pharmacophore. ΔE_1 values were obtained from energy differences between lowest energy conformer and superposition conformers of indicated compounds onto the four-point pharmacophore.

Compound	Inhibition at 100 (μg/ml)		IC_{50}		Antiviral activity		RMS	ΔE_1
	3′-Processing	Strand transfer	3′-Processing	Strand transfer	IC_{50}	EC_{50}		
	%		μM		μM		Å	Kcal/mol
1 NSC 309121			1.7 ± 0.7	1.0 ± 0.3			0.342	0.82
2 NSC 318213			23.9 ± 0.7	14.0 ± 7.0			0.324	1.73
3 NSC 607319			1.4 ± 1.4	1.0 ± 1.0	21.1	>21.1	0.481	0.33
4 NSC 281311	35.5	44.1	>200	>200			0.589	13.67
5 NSC 324982	57.7	30.9			>100	>100	0.542	23.46
6 NSC 332542	81.2	84.6	104.4 ± 21.3	32.0 ± 17.7			0.206	2.60
7 NSC 359095	49.9	49.9	294	294	>200	>200	0.398	12.72
8 NSC 505719	76.5	72.8	66.8 ± 18.0	76.7 ± 27.4			0.376	0.79
9 NSC 632823	37.3	35.8	>200	>200	>127	>127	0.508	3.98
10 NSC 636681	42.0	50.3	>200	200	>165	>165	0.432	8.58
11 NSC 624404			1.4 ± 0.4	2.3 ± 2.1	11.7	>11.7	0.451	0.39
12 NSC 642651	35.5	47.1	>160	>160	78	>78	0.513	6.14
13 NSC 371835			15.9 ± 1.9	16.6 ± 0.6	3.3	>3.3	0.465	0.13
14 NSC 674503	42.2	45.7	>180	>180	3.3	>3.3	0.350	1.53
15 NSC 674504	52.9	40.5			3.4	>3.4	0.555	5.12
16 NSC 248605	50.0	50.0	140	140	0.3	>0.3	0.410	7.96
17 NSC 328421	21.5	27.0	>130	>130	4.3	>4.3	0.589	11.86
18 NSC 192709	25.1	12.7	>200	>200			0.515	5.12
19 NSC 600267	12.8	14.2	>170	>170	>100	>100	0.455	2.38
20 NSC 369085	41.9	37.4	>160	>160			0.467	6.98
21 NSC 233026			20.6 ± 8.3	19.7 ± 0.5	7.7	>7.7	0.406	0.00
22 NSC 354646			1.4 ± 0.4	1.5 ± 0.7			0.372	0.00
23 NSC 261045			2.3 ± 0.8	4.1 ± 2.0	>0.2	>0.2	0.488	0.73
24 NSC 267583	25.5	20.1	>100	>100			0.492	1.28
25 Tetracycline			204.0 ± 37.4	188.0 ± 30.8	40.5	>40.5	0.410	0.05
26 Rolitetracycline			28.0 ± 22.5	34.1 ± 13.3	45.5	>45.5	0.387	0.00
27 NSC 43891			1.7 ± 1.2	1.1 ± 0.5			0.418	0.67
28 NSC 43889			2.2 ± 0.9	2.8 ± 2.0	>268	>268	0.296	0.00
29 NSC 56714			1.9 ± 0.9	1.9 ± 0.2			0.346	0.00
30 NSC 56712			3.5 ± 1.3	3.0 ± 1.5			0.410	0.02
31 NSC 64205			1.1 ± 0.6	0.5 ± 0.3	34.3	>34.3	0.389	0.00
32 NSC 64431			1.2 ± 0.7	1.7 ± 1.0	100	>100	0.389	0.00
33 NSC 64452			1.2 ± 0.2	3.6 ± 1.8	120	>120	0.410	0.04
34 NSC 67586			1.3 ± 1.0	2.1 ± 0.3	0.6	>0.6	0.363	0.00
35 NSC 69318			1.6 ± 1.4	0.3 ± 0.1	100	>100	0.389	0.00
36 NSC 69319			1.3 ± 0.4	1.6 ± 0.6	133	>133	0.389	0.00
37 NSC 69326			5.1	2.5	>111	>111	0.365	0.00
38 NSC 69345			1.3 ± 0.2	1.0 ± 0.3	>37	>37	0.410	0.02
39 NSC 118695			0.9 ± 0.6	0.3 ± 0.1	0.3	>0.3	0.252	0.00

for the importance of both conformational energy and geometric fit. However, no linear relationship was established between F and the IC_{50} value. This is reasonable because conformational energy penalty and geometric fitness of a pharmacophore in binding conformation are only two of the factors that influence the activity of an inhibitor; other properties, such as hydrophobicity and steric and electronic factors, also should be considered for each inhibitor.

Selection of compounds that contain the four-point pharmacophore. Structures of the 39 four-point pharmacophore-containing compounds assayed in this study are shown in Fig. 4. The pharmacophore query was built on the basis of the hydrogen bond donating capabilities of the inhibitors because in many cases, the hydrogen bond interaction provides a major contribution to the overall free energy of binding. Because a basic nitrogen may be capable of behaving as either a hydrogen bond donor or acceptor, a basic nitrogen atom was allowed in place of oxygen in the search, and several of the retrieved compounds (e.g., **6**, **8**, **12**, **13**, **15**, **19**, **21–24**, and **25–39**) contain at least one basic nitrogen atom in the pharmacophore assembly.

***In vitro* inhibition of HIV-1 IN.** Catechol-containing compounds in general are potent inhibitors of IN *in vitro* (1). In many instances, this inhibition is associated with nonspecific binding to other cellular targets. Thus, collateral toxicity associated with this class of inhibitors is of major concern in anti-HIV drug development. We have used 3D database searching of the National Cancer Institute drug screening program to identify novel inhibitors of IN and identified novel non-catechol-containing inhibitors (1), some of which are presented in this study. Several of the inhibitors reported are analogs of compounds reported previously; for example, we identified a series of flavones as inhibitors of IN (25). Novel flavones, such as the dihydrochalcone derivative **1** and the phylloflavan **3**, inhibited IN <2 μM. In common with the chicoric and caffeoylquinic acids, compounds **1–3** contain two catechol moieties. All of the catechol-containing compounds exhibited similar potency as those for the chicoric and caf-

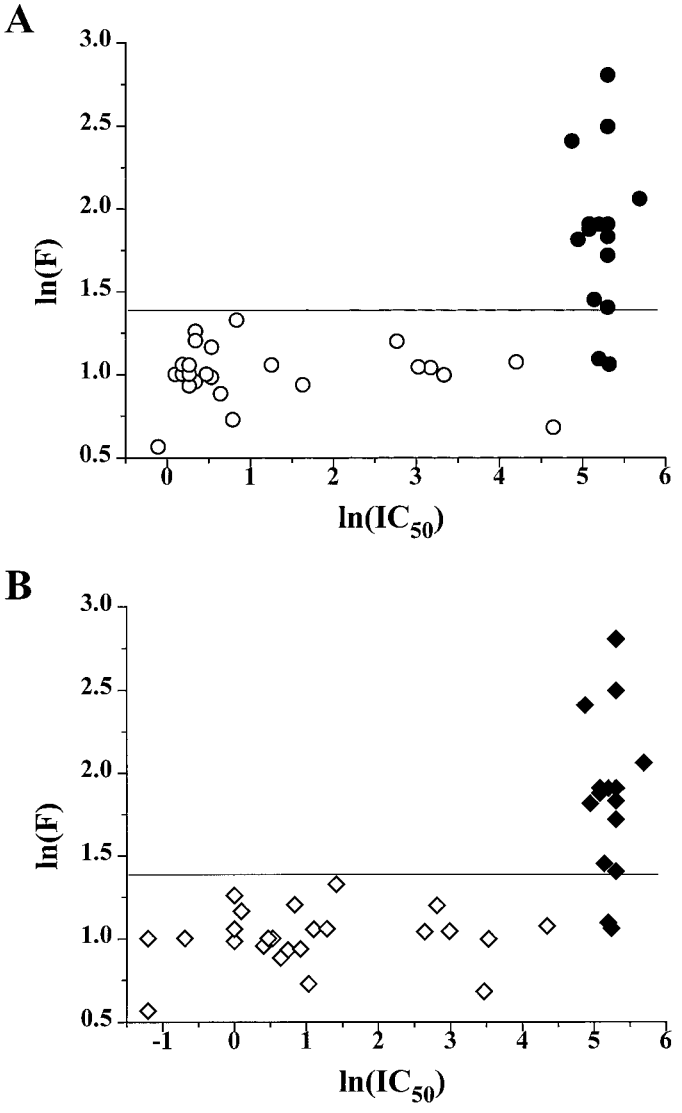

Fig. 5. Correlation between HIV-1 integrase inhibitory potency and F values according to the equation $F = (\Delta E_1 - \Delta E_2)(RMS)$. The natural logarithm of IC_{50} values for 3′-processing (A) and strand transfer (B) is plotted against the natural logarithm of F.

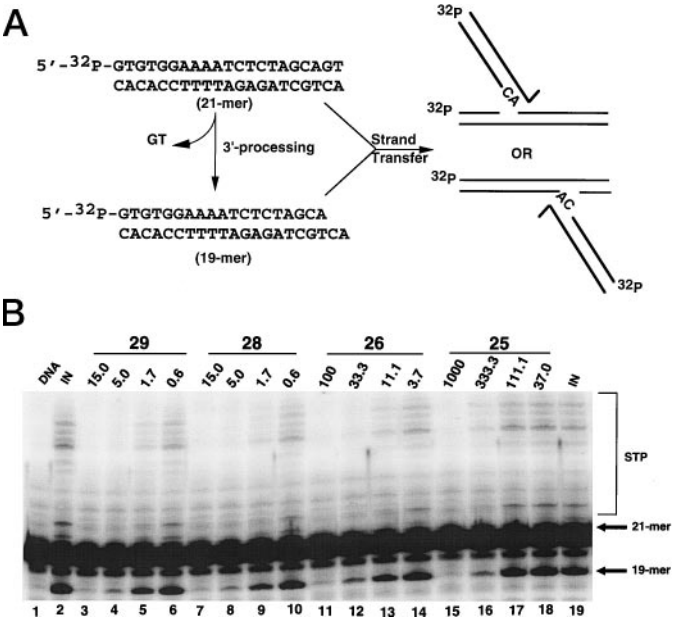

Fig. 6. HIV-1 integrase catalytic assays. A, A 21-mer blunt-end oligonucleotide that corresponds to the U5 end of the HIV-1 proviral DNA, 5′-end-labeled with ^{32}P, is reacted with purified HIV-1 integrase. The initial step involves nucleolytic cleavage of two bases from the 3′-end, which results in a 19-mer oligonucleotide. Subsequently, 3′-ends are covalently joined to another identical oligonucleotide, which serves as the target DNA. B, Concentration-dependent inhibition of HIV-1 IN by tetracyclines **29, 28, 26**, and **25**. *Above each lane,* drug concentrations in micromolar.

feoylquinic acids, apparently regardless of the linker length and linker geometry. Compound **11**, with two seven-membered rings, also exhibited remarkable potency, with IC_{50} values of 1.4 and 2.3 μM for 3′-processing and strand transfer, respectively. However, when the OH groups are protected, as in compounds **9**, **10**, and **20**, total loss of activity was observed (Table 1). These results are in accord with our recent investigation of a series of monohydroxylated arylamide inhibitors of IN (26). Derivatization of a hydroxyl group in a series of catechol-containing inhibitors abolished anti-IN activities (26), and the implication is that a hydrogen bond donor (—OH) is necessary at these positions: a hydrogen bond acceptor (—O—) is inadequate. Anthracycline antibiotics **22** and **23** exhibited IC_{50} values of 1.4 ± 0.4 and 2.3 ± 0.8 μM for 3′-processing and 1.5 ± 0.7 and 4.1 ± 2.0 μM for strand transfer, respectively. In accord with our earlier observations (27), several other anthracyclines also showed similar potency range (data not shown). *N*-Caffeoylglycine-L-phenylalanine (**6**), with IC_{50} values of 104.4 ± 21.3 μM for 3′-processing and 32.0 ± 17.7 μM for strand transfer, was moderately active. The disulfides **7** and **8** exhibited moderate activity, whereas the sulfonylamides **14** and **15** were less active.

Compounds **4**, **5**, **12**, and **14–20** were all inactive, but compounds **13** and **21** exhibited IC_{50} values of 16 and 20 μM for 3′-processing, respectively. In the tetracycline series of compounds, the parent tetracycline **25**, with IC_{50} values of 204.0 ± 37.4 and 188.0 ± 30.8 μM for 3′-processing and strand transfer, exhibited marginal potency against IN. However, pyrrolidinyl methyl substitution at carboxamide group to protect the free amine increased the potency 5-fold. This increase in potency was seen in all other substituted tetracyclines, **27–39**. Thus, tetracyclines **27–39** were equally potent, with an IC_{50} range of 1.0–5.0 μM for both 3′-processing and strand transfer. The tetracyclines presented in this study are a new class of IN inhibitors and were examined further in different assays to probe the site and specificity of their inhibitory action.

Relevance to antiviral activity. We based our study on the caffeoylquinic and chicoric acids that had been reported to exhibit antiviral activity with high potency against IN (3, 4). Interestingly, none of the caffeoylquinic acids tested in the National Cancer Institute Antiviral Drug Screening Program exhibited detectable activity against HIV-1-infected CEM cells (10). In addition, none of the tested compounds presented in Table 1 exhibited significant antiviral activity. Compounds **13–17**, **21**, **34**, and **39** showed remarkable cytotoxicity. Interestingly, several of the tetracyclines were noncytotoxic, which suggests that they are devoid of nonspecific cellular effects. Further rational drug design requires synthesis of derivatives that would be more stable by modifying the *R* group (Fig. 4) to prevent intracellular cleavage, leading

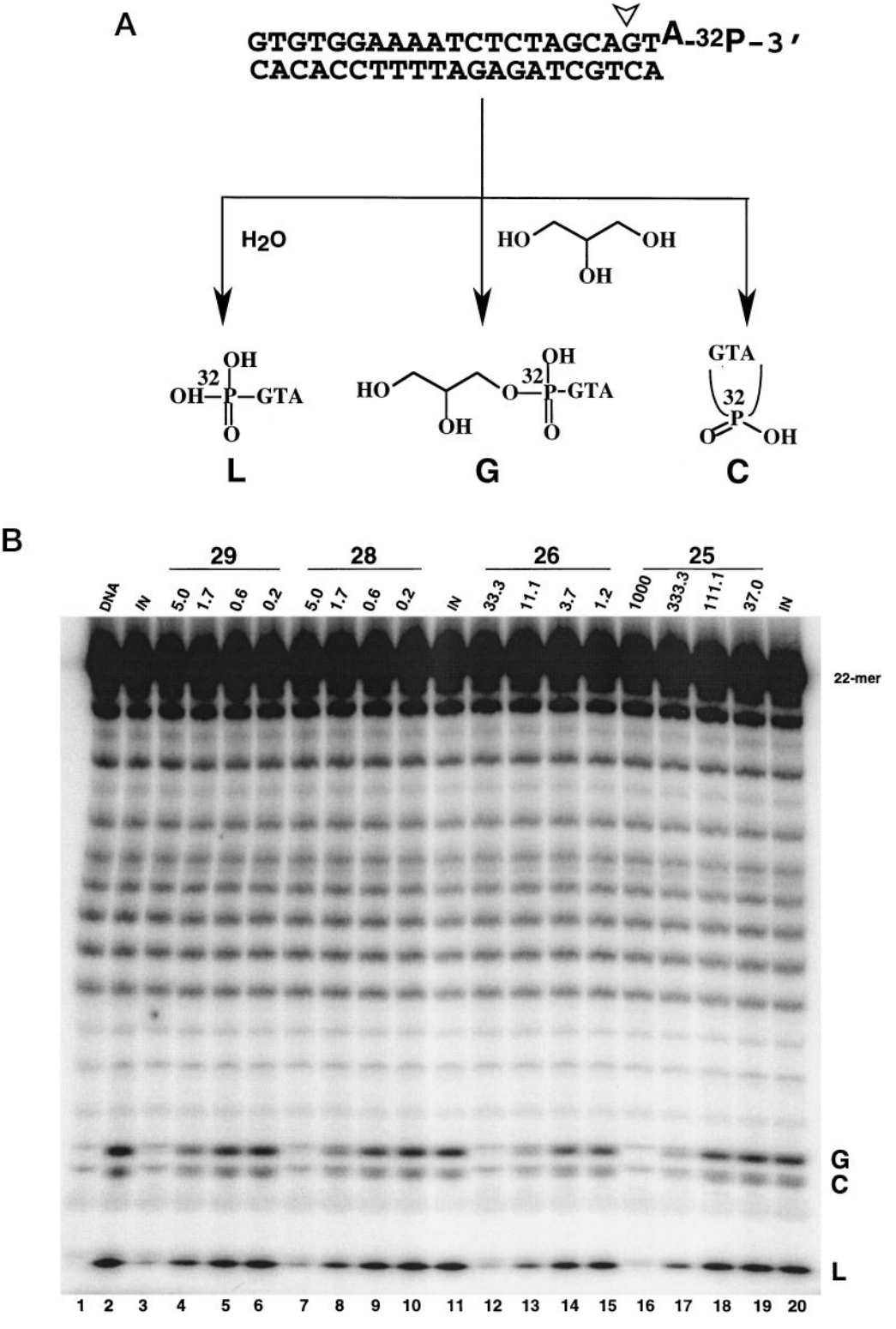

Fig. 7. Choice of nucleophile for the 3′-processing reaction by HIV-1 integrase. A, Nucleophilic substitution of water, glycerol, or the 3′-hydroxyl group of the viral DNA terminus yielding a linear trinucleotide with a 5′-phosphate (*L*), a linear trinucleotide with a glycerol esterified to the 5′-phosphate (*G*), and a cyclic trinucleotide (*C*). Global inhibition of nucleophilic attack in the 3′-processing reaction by tetracyclines **29**, **28**, **26**, and **25** (B). *Above each lane,* drug concentrations in micromolar.

to the parent tetracycline, which has only marginal potency against IN.

Although some hydroxylated aromatics may have antiviral activities, their *in vivo* selectivity against IN remains to be established. However, there is increasing evidence for their nonselective binding to other targets. For example, in a recent study, Natarajan *et al.* (28) showed that caffeic acid phenethyl ester is a potent and specific inhibitor of nuclear factor-κB activation induced by different agents (28). Moreover, NDGA and 3-*O*-methyl-NDGA were reported to inhibit HIV-1 transcription and replication by inhibiting HIV-1 Tat function (29). In our *in vitro* assay, NDGA also exhibited moderate potency against purified IN.[1] A recent report by Baxter *et al.* (30) indicates that multiple interactions be-

[1] N. Neamati and Y. Pommier, unpublished observations.

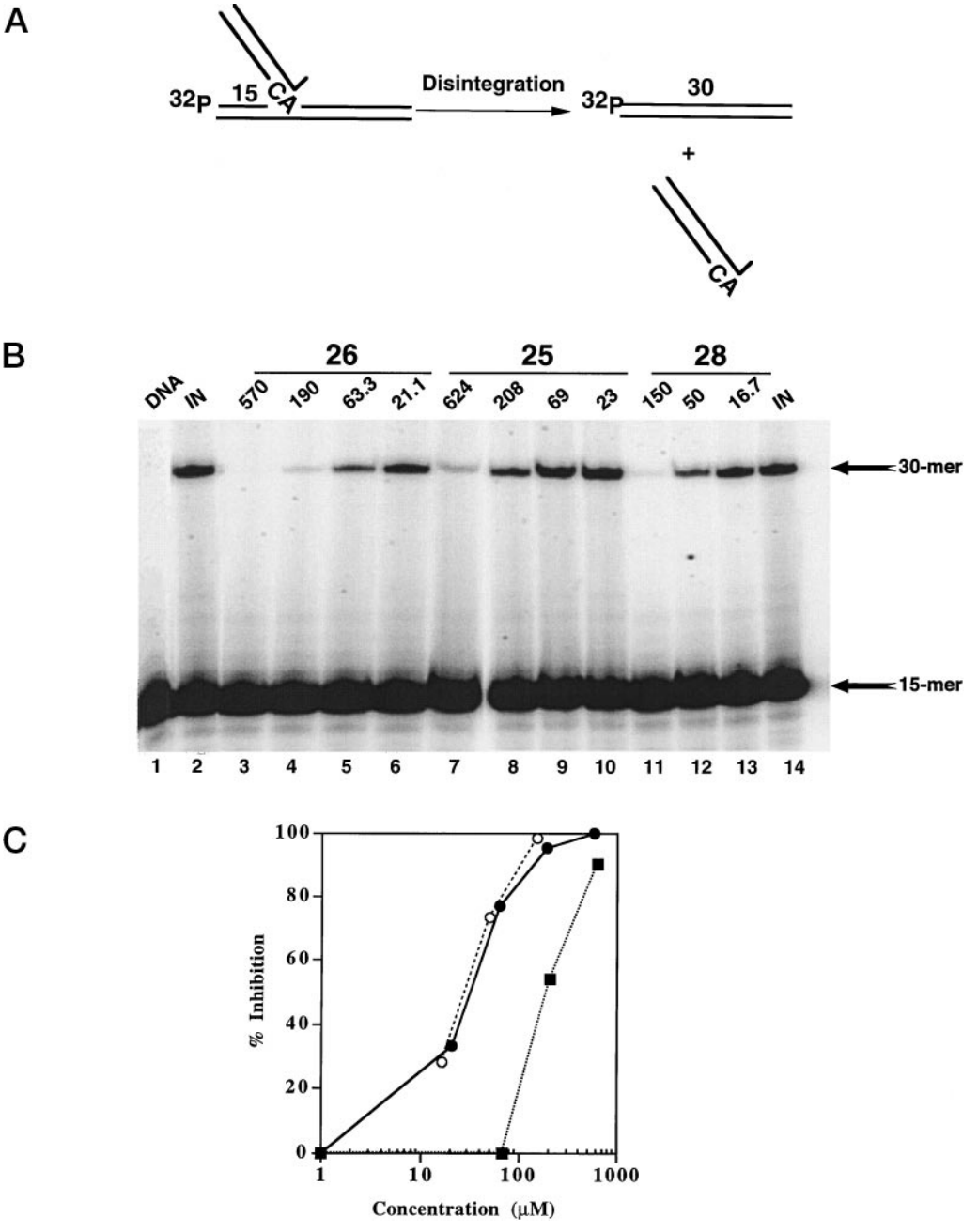

Fig. 8. HIV-1 integrase disintegration assay using the IN core domain. A, The substrate oligonucleotide mimics a strand transfer step product (i.e., a Y oligonucleotide that contains a 15-mer oligonucleotide 5′-end-labeled with ^{32}P). HIV-1 integrase mediates the disintegration generating a 30-mer oligonucleotide. B, Concentration-dependent inhibition of IN^{50-212} (F185K)-catalyzed disintegration step by compounds **26**, **25** and **28.** The electrophoresis in a 20% denaturing acrylamide gels showing the original 15-mer and the 30-mer disintegration products. *Above each lane,* drug concentrations in micromolar. C, Graph that shows the quantification of results in B. *25*, ○; *26*, ●; *28*, ■. Percent inhibition was calculated after PhosphorImager quantification.

tween polyphenols and a salivary proline-rich protein repeat resulted in complexation and precipitation. Thus, the propensity to form nonspecific complexes with proteins, DNA, and polysaccharides remains a major concern in the development of polyphenolic-based inhibitors. This lack of specificity in combination with poor cellular uptake translates into poor antiviral activity in cell-based assays. Nevertheless, the use of potent inhibitors as drug lead is of major impetus in development of a more selective inhibitor.

Mechanism of IN inhibition by tetracyclines. On infection of cells, effective retroviral replication requires the integration of a double-stranded DNA copy of the viral single-stranded RNA genome into a host chromosome. HIV-1 IN is known to catalyze two consecutive reactions. Initially, it processes linear viral DNA by removing the nucleotides 3′ from the conserved CA, leaving the recessed 3′-OH termini. Subsequently, the processed 3′-ends of the viral DNA are then covalently joined to host DNA (1, 31, 32). These two steps, known respectively as 3′-processing and DNA strand transfer, can be readily measured in an *in vitro* assay using purified recombinant IN, a 21-mer duplex oligonucleotide that corresponds to the U5 end of the HIV long terminal repeat sequence (Fig. 6A) and divalent metal ion (Mn^{2+} or Mg^{2+}). Fig. 6B shows a representative gel that illustrates inhibition of both 3′-processing and strand transfer reactions by tetracyclines **29**, **28**, **26**, and **25**. The substituted tetracyclines **26**, **28**, and **29** were 5–100-fold more potent than the parent compound **25**. When we examined the inhibition of 3′-processing and strand transfer in the presence of Mg^{2+}, no significant differences in IC_{50} values were observed from those in the presence of Mn^{2+} (not shown). The IC_{50} values for 3′-processing and strand transfer, respectively, were 2.7

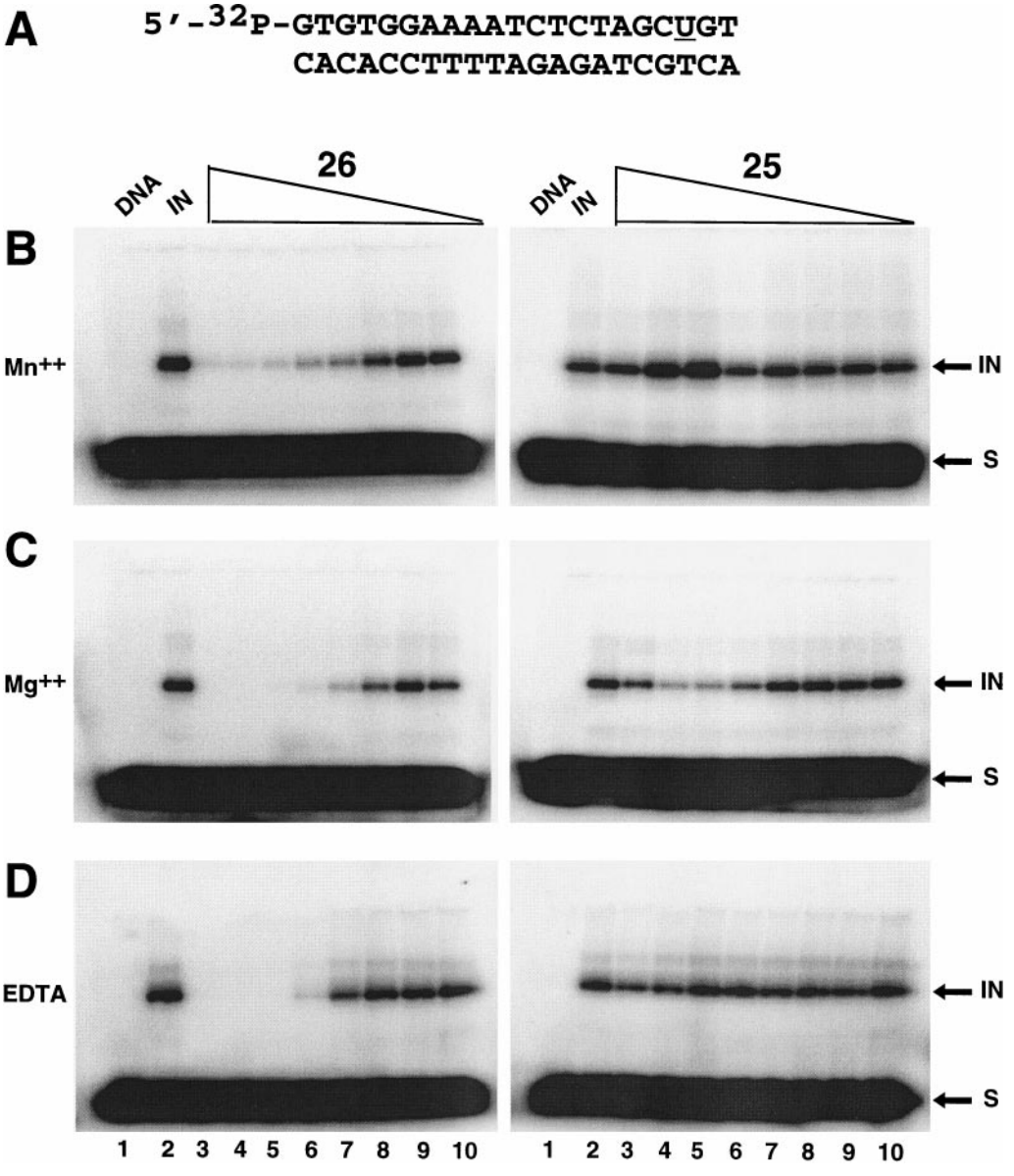

Fig. 9. IN-DNA cross-linking by formation of a Schiff base between IN and a duplex oligonucleotide that contains an abasic site. A, A 21-mer blunt-end oligonucleotide that corresponds to the U5 end of HIV proviral DNA that contains a uracil (*underlined*) in place of an adenine. B, Effect of tetracycline **25** and rolitetracycline **26** on the extent of DNA binding of HIV-1 integrase in the presence of 2 mM manganese chloride (A), 2 mM magnesium chloride (B), or 2 mM EDTA (C). PhosphorImager image that shows the inhibition of the 39-kDa product that corresponds to the IN-DNA covalent complex (*lane 2*) in the presence of 1000, 250, 100, 50, 25, 10, and 1 μM concentration of drugs (*lanes 3-10*).

and 2.4 μM for **29**, 3.2 and 3.1 μM for **28**, 49.8 and 43.2 μM for **26**, and 341.0 and 333.0 μM for **25.**

The 3′-processing reaction involves hydrolysis of a single phosphodiester bond 3′ of the conserved CA-3′ dinucleotide. However, in addition to this hydrolysis reaction, retroviral integrases can use glycerol or the hydroxyl group of the viral DNA terminus as the nucleophile in the 3′-processing reaction, which yields a glycerol esterified to the 5′-phosphate, or a circular dinucleotide or trinucleotide, respectively (33–35) (Fig. 6A). To examine the effect of several inhibitors on the choice of nucleophiles in the 3′-processing reaction, a substrate DNA labeled at the 3′-end was used (34). Tetracyclines **29**, **28**, **26**, and **25** inhibited glycerolysis, hydrolysis, and circular nucleotide formation (Fig. 7B) to essentially the same extent, consistent with the data shown in Fig. 6B.

In addition to the 3′-processing and strand transfer reactions described above, IN can catalyze reversal of strand transfer, which leads to the "disintegration" step shown in Fig. 8A (16). One of the interesting aspect of the disintegration reaction is that an IN deletion mutant $IN^{50–212}$ lacking both the amino-terminal zinc binding and the carboxyl-terminal DNA binding domains remains active in this assay, whereas such truncated IN loses activity in the 3′-processing and strand transfer assays (16). Thus, the disintegration assay can be used to probe the site of drug-enzyme binding. We have used two core mutants, $IN^{50–212}$ wild-type or a soluble $IN^{50–212}$ (F185K) mutant (36), in this assay and a Y oligonucleotide that mimics a strand-transfer product (Fig. 8A). As shown in Fig. 8B, tetracyclines **25**, **26,** and **28** inhibited disintegration by $IN^{50–212}$ (F185K) with IC_{50} values of 197, 36.9, and 29.7 μM, respectively, which implies that the IN core domain is sufficient for inhibition and that binding of tetracyclines to the IN core region is responsible for IN inhibition.

The catalytic domain of HIV-1 IN (amino acids 50–212) is characterized by the D, D(35)E motif, in which the invariable aspartic acid residues (D) are located at positions 64 and 116, and the glutamic acid residue (E) is located at position 152. It has also been well established that integrases require a divalent cation as a cofactor for catalysis and that the divalent

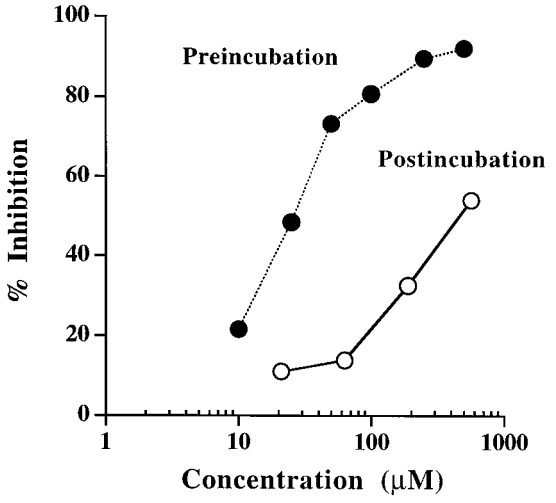

Fig. 10. Concentration- and time-dependent inhibition of IN-DNA binding by rolitetracycline **26.** Preincubation indicates that drug was incubated with the enzyme for 30 min before the addition of DNA. Postincubation indicates that drug was added 5 min after IN and DNA were mixed. Reaction was performed in the presence of 2 mM manganese chloride.

metal ion probably binds to the D, D(35)E motif (31, 32, 37). Because tetracyclines are potent chelating agents, they might participate in the extraction of the metal ions from the IN binding site. However, the chelation properties of tetracyclines might not account for the differences in their IN inhibition. For example, the parent tetracycline (**25**) exhibited IC_{50} values of 204.0 ± 37.4 and 188.0 ± 30.8 μM for 3′-processing and strand transfer, respectively, whereas rolitetracycline (**26**), with IC_{50} values of 28.0 ± 22.5 and 34.1 ± 13.3 μM for 3′-processing and strand transfer, respectively, was 5 times more potent than the parent compound (Table 1). An even further increase in potency is observed as the bulk of the substituent on the carboxamide moiety at C2 increases. Three other commercially available tetracycline analogs that contain the free carboxamide group (oxytetracycline, doxycycline, and methacycline) were also tested in our IN inhibition assay and found to exhibit potencies in the same range as the tetracycline **25** (data not shown). The obvious difference was the presence of a protecting group on the carboxamide group. Whether these subtle differences could play a major contribution to metal binding is not clear; however, there are precedents for differential metal binding characteristics of tetracycline in solution (38, 39).

To determine the role of metal binding and potentially explain the difference in IC_{50} values of tetracycline and rolitetracycline, we examined the effect of DNA binding by IN in the presence of divalent metal (Mn^{2+} or Mg^{2+}) or in the absence of metal in the presence of EDTA. Using a recently described assay (13) to trap the IN on a DNA substrate that contains an abasic site, we demonstrated that rolitetracycline (**26**) inhibits IN-DNA binding and that this inhibition is metal independent. The tetracycline **25** was markedly less potent inhibitor of IN binding to DNA (Fig. 9), which is consistent with the greater activity of rolitetracycline (**26**) over tetracycline (**25**) in the 3′-processing, strand transfer, and disintegration assays described above. We also found that rolitetracycline inhibited the IN^{50-212} core binding to DNA, which is consistent with the results of functional assays (Figs. 6–8) and indicates that tetracyclines act on the IN catalytic core. Together, these results indicate that tetracyclines inhibit IN, presumably by acting on the IN catalytic core domain. Results of IN-DNA binding experiments suggest that this effect does not require Mn^{2+} or Mg^{2+} cofactor.

It has been established that IN rapidly forms a stable complex with its DNA substrate and that this complex has not been shown to reverse with any of the known inhibitors. Interestingly, rolitetracycline (**26**) was able to displace DNA from the IN after the complex was allowed to form 5 min before the addition of the drug (Fig. 10, postincubation). However, ≥15-fold more drug was required for 50% inhibition. When drug was incubated 30 min before the addition of DNA (Fig. 10, preincubation), an IC_{50} value of 37 μM was obtained. Accordingly, a higher concentration of rolitetracycline (**26**) was required to inhibit DNA binding using IN^{50-212} (F185K) mutant (data not shown). Nevertheless, to inhibit all three IN enzymatic activities, only ≤37 μM was required to achieve 50% inhibition (Figs. 6B, 7B, and 8B).

Tetracyclines do not affect eukaryotic DNA topoisomerase I. Eukaryotic topoisomerase I assays can be used to probe the selectivity of compounds toward other DNA binding proteins. To determine the extent of topoisomerase I cleavable complex formation and inhibition of cleavable complex trapped by camptothecin, a 33-mer oligonucleotide bear-

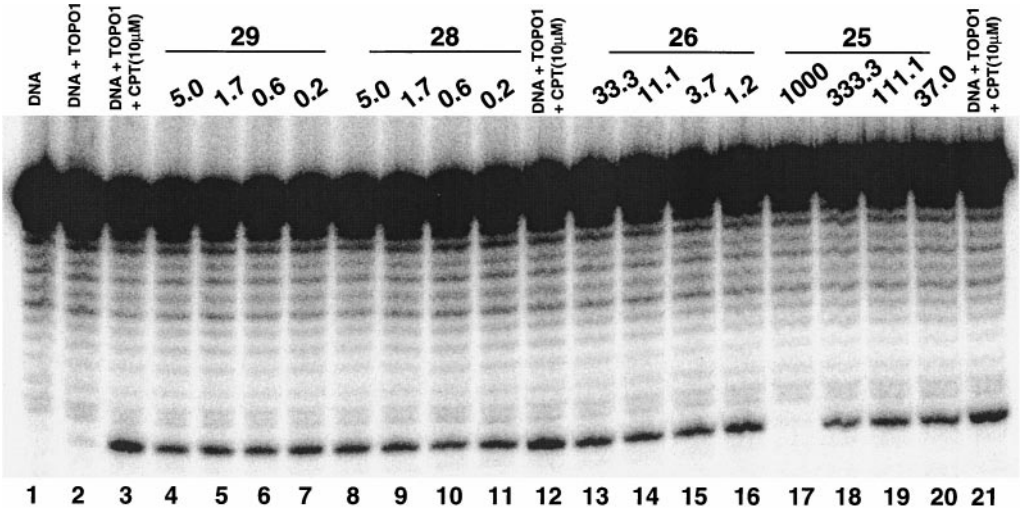

Fig. 11. Inhibition of camptothecin-induced cleavable complex formation by compounds **29**, **28**, **26**, and **25**. *Lane 1*, DNA alone. *Lane 2*, DNA plus topoisomerase I. *Lanes 3–21*, DNA and topoisomerase I plus camptothecin (10 μM); *numbers above lanes*, drug concentration in micromolar.

ing a unique topoisomerase I cleavage site in its center was used (17). and formation of the cleavable complex was monitored. None of the four tetracyclines (**29**, **28**, **26**, and **25**) tested induced any detectable cleavable complex (data not shown) or inhibited the ability of topoisomerase I to generate camptothecin-mediated cleavable complex at concentrations that effectively inhibited IN (Fig. 11). These results indicate that the tested compounds exhibit some selectivity for IN and suggest that their inhibitory potency is not due to nonspecific binding to the IN or the DNA. Compounds **29**, **28**, and **26** exhibited no significant inhibition at the highest concentration tested, and tetracycline **25** showed an IC_{50} value of 400 μM against topoisomerase I (Fig. 11).

We also tested tetracyclines **29**, **28**, **26**, and **25** against recombinant HIV-2 integrase; IC_{50} values were similar to those for HIV-1 integrase. The IC_{50} values for 3′-processing and strand transfer, respectively, were 4.4 and 3.8 μM for **29**, 4.3 and 4.2 μM for **28**, 10.4 and 9.3 μM for **26**, and 227.0 and 243.0 μM for **25.**

Tetracycline as lead compounds. A unique class of compounds identified in this study are the tetracyclines **25–39**, which inhibited IN at low micromolar concentrations. Tetracyclines reported in this study are water soluble and potential candidates for cocrystallization with wild-type IN. In addition, tetracyclines are strong chelating agents and therefore of interest in elucidating the role of metal ions in the mechanism of IN function. It is puzzling why the prototype tetracycline with no substituent on the carboxamide group at the 2 position is considerably less potent than the carboxamido protected derivatives. This disparity is perhaps partially due to the nature of chelating properties of the tetracyclines. Alternatively, substituted tetracyclines could undergo intramolecular rearrangement on the side group (*R* group in Fig. 4) to release reactive electrophiles at the IN catalytic site. Although all the structures presented in this study contain the four-point pharmacophores, which can reasonably be superimposed on one another, the requirement for potency against IN is stringent, and subtle changes in structure can greatly affect their potency. Therefore, a more precise pharmacophore determination may have to await X-ray or NMR structural information. We are currently engaged in determining the cocrystal structure of several of the water-soluble inhibitors with HIV-1 IN.

References

1. Pommier, Y., A. Pilon, K. Bajaj, A. Mazumder, and N. Neamati. HIV-1 integrase as a target for antiviral drugs. *Antiviral Chem. Chemother.* **8:** 483–503 (1997).
2. Neamati, N., S. Sunder, and Y. Pommier. Design and discovery of HIV-1 integrase inhibitors. *Drug Discovery Today* **2:** 487–498 (1997).
3. Robinson, W. E., Jr., M. Cordeiro, S. Abdel-Malek, Q. Jia, S. A. Chow, M. G. Reinecke, and W. M. Mitchell. Dicaffeoylquinic acid inhibitors of human immunodeficiency virus integrase: inhibition of the core catalytic domain of human immunodeficiency virus integrase. *Mol. Pharmacol.* **50:**846–855 (1996).
4. Robinson, W. E., Jr., M. G. Reinecke, S. Abdel-Malek, Q. Jia, and S. A. Chow. Inhibitors of HIV-1 replication that inhibit HIV integrase. *Proc. Natl. Acad. Sci. USA* **93:**6326–3631 (1996).
5. Scarpati, M. L., and G. Oriente. Chicoric acid (dicaffeyltartic acid): its isolation from chicory (*Chicorium intybus*) and synthesis. *Tetrahedron* **4:**43–48 (1958).
6. Cheminat, A., R. Zawatzky, H. Becker, and R. Brouillard. Caffeoyl conjugates from echinacea species: structures and biological activity. *Phytochemistry* **27:**2782–2794 (1988).
7. Mahmood, N., P. S. Moore, N. De Tommasi, F. De Simone, S. Colman, A. J. Hay, and C. Pizza. Inhibition of HIV infection by caffeoylquinic acid derivatives. *Antiviral. Chem. Chemother.* **4:**235–240 (1993).
8. Parker, W. B., M. Nishizawa, M. H. Fisher, N. Ye, K.-H. Lee, and Y.-C. Cheng. Characterization of a novel inhibitor of human DNA polymerases: 3,4,5-tri-O- galloylquinic acid. *Biochem. Pharmacol.* **38:**3759–3765 (1989).
9. Rice-Evans, C. Plant polyphenols: free radical scavenger or chain-breaking antioxidants? *Biochem. Soc. Symp.* **61:**103–116 (1995).
10. Neamati, N., H. Hong, A. Mazumder, S. Wang, S. Sunder, M. C. Nicklaus, G. W. A. Milne, B. Proksa, and Y. Pommier. Depsides and depsidones as inhibitors of HIV-1 integrase: discovery of novel inhibitors through 3D database searching. *J. Med. Chem.* **40:**942–951 (1997).
11. Nicklaus, M. C., N. Neamati, H. Hong, A. Mazumder, S. Sunder, J. Chen, G. W. A. Milne, and Y. Pommier. HIV-1 integrase pharmacophore: discovery of inhibitors through 3D database searching. *J. Med. Chem.* **40:**920–929 (1997).
12. Hong, H., N. Neamati, S. Wang, M. C. Nicklaus, A. Mazumder, Y. Pommier, H. Zhao, J. T. R. Burke, and G. W. A. Milne. Discovery of HIV-1 integrase inhibitors by pharmacophore searching. *J. Med. Chem.* **40:**930–936 (1997).
13. Mazumder, A., N. Neamati, A. A. Pilon, S. Sunder, and Y. Pommier. Chemical trapping of ternary complexes of human immunodeficiency virus type 1 integrase, divalent metal, and DNA substrates containing an abasic site: implications for the role of lysine 136 in DNA binding. *J. Biol. Chem.* **271:**27330–27338 (1996).
14. Mazumder, A., N. Neamati, S. Sunder, J. Owen, and Y. Pommier. Retroviral integrase: a novel target in antiviral development; basic in vitro assays with the purified enzyme, in *Methods in Cellular and Molecular Biology: Antiviral Evaluation* (D. Kinchington and R. Schinazi, eds.). The Humana Press, Totowa, NJ, in press.
15. Mazumder, A., N. Neamati, J. P. Sommadossi, G. Gosselin, R. F. Schinazi, J. L. Imbach, and Y. Pommier. Effects of nucleotide analogues on human immunodeficiency virus type 1 integrase. *Mol. Pharmacol.* **49:**621–8 (1996).
16. Chow, S. A., K. A. Vincent, V. Ellison, and P. O. Brown. Reversal of integration and DNA splicing mediated by integrase of human immunodeficiency virus. *Science (Washington D. C.)* **255:**723–726 (1992).
17. Pommier, Y., G. Kohlhagen, K. W. Kohn, F. Leteurtre, M. C. Wani, and M. E. Wall. Interaction of an alkylating camptothecin derivative with a DNA base at topoisomerase 1-DNA cleavage sites. *Proc. Natl. Acad. Sci. USA* **92:**8861–8865 (1995).
18. Milne, G. W. A., M. C. Nicklaus, J. S. Driscoll, S. Wang, and D. W. Zaharevitz. The NCI drug information system 3D database. *J. Chem. Inf. Comput. Sci.* **34:**1219–1224 (1994).
19. Milne, G. W. A., and J. A. Miller. The NCI drug information system. *J. Chem. Inf. Comput. Sci.* **26:**154–197 (1986).
20. Milne, G. W. A., S. Wang, and M. C. Nicklaus. Molecular modeling in the discovery of drug leads. *J. Chem. Inf. Comput. Sci.* **36:**726–730 (1996).
21. Wang, S., D. W. Zaharevitz, R. Sharma, V. E. Marquez, N. E. Lewin, L. Du, P. M. Blumberg, and G. W. A. Milne. The discovery of novel, structurally diverse protein kinase C agonists through computer 3D-database search: molecular modeling studies. *J. Med. Chem.* **37:**4479–4489 (1994).
22. Wang, S., G. W. A. Milne, X. Yan, I. Posey, M. C. Nicklaus, L. Graham, and W. G. Rice. Discovery of novel, non-peptide HIV-1 protease inhibitors by pharmacophore searching. *J. Med. Chem.* **39:**2047–2054 (1996).
23. Brooks, B. R., R. E. Bruccoleri, B. D. Olafson, D. J. States, S. Swaminathan, and M. Karplus. CHARMm: a program for macromolecular energy minimization and dynamics calculations. *J. Comput. Chem.* **4:**187–217 (1983).
24. Nicklaus, M. C., S. Wang, J. S. Driscoll, and G. W. A. Milne. Conformational changes of small molecules binding to proteins. *Bioorg. Med. Chem.* **3:**411–428 (1995).
25. Fesen, M. R., Y. Pommier, F. Leteurtre, S. Hiroguchi, J. Yung, and K. W. Kohn. Inhibition of HIV-1 integrase by flavones, caffeic acid phenethyl ester (CAPE) and related compounds. *Biochem. Pharmacol.* **48:**595–608 (1994).
26. Zhao, H., N. Neamati, A. Mazumder, S. Sunder, Y. Pommier, and T. R. Burke, Jr. Arylamide inhibitors of HIV-1 integrase. *J. Med. Chem.* **40:** 1186–1194 (1997).
27. Fesen, M. R., K. W. Kohn, F. Leteurtre, and Y. Pommier. Inhibitors of human immunodeficiency virus integrase. *Proc. Natl. Acad. Sci. USA* **90:**2399–403 (1993).
28. Natarajan, K., S. Singh, T. R. Burke, D. Grunberger, and B. B. Aggarwal. Caffeic acid phenethyl ester is a potent and specific inhibitor of activation of nuclear transcription factor NF-κB. *Proc. Natl. Acad. Sci. USA* **93:**9090–9095 (1996).
29. Gnabre, J. N., J. N. Brady, D. J. Clanton, Y. Ito, J. Dittmer, R. B. Bates, and R. C. C. Huang. Inhibition of human immunodeficiency virus type 1 transcription and replication by DNA sequence-selective plant lignans. *Proc. Natl. Acad. Sci. USA* **92:**11239–11243 (1995).
30. Baxter, N. J., T. H. Lilley, E. Haslam, and M. P. Williamson. Multiple interaction between polyphenols and a salivary proline-rich protein repeat results in complexation and precipitation. *Bichemistry* **36:**5566–5577 (1997).
31. Rice, P., R. Craigie, and D. R. Davies. Retroviral integrases and their cousins. *Curr. Opin. Struct. Biol.* **6:**76–83 (1996).
32. Katz, R. A., and A. M. Skalka. The retroviral enzymes. *Annu. Rev. Biochem.* **63:**133–173 (1994).
33. Engelman, A., K. Mizuuchi, and R. Craigie. HIV-1 DNA integration: mech-

anism of viral DNA cleavage and DNA strand transfer. *Cell* **67:**1211–1221 (1991).
34. Mazumder, A., S. Wang, N. Neamati, M. Nicklaus, S. Sunder, J. Chen, G. W. Milne, W. G. Rice, T. R. Burke, Jr., and Y. Pommier. Antiretroviral agents as inhibitors of both human immunodeficiency virus type 1 integrase and protease. *J. Med. Chem.* **39:**2472–2481 (1996).
35. Vink, C., E. Yeheskiely, G. A. van der Marel, J. H. van Boom, and R. H. Plasterk. Site-specific hydrolysis and alcoholysis of human immunodeficiency virus DNA termini mediated by the viral integrase protein. *Nucleic Acids Res.* **19:**6691–6698 (1991).
36. Jenkins, T. M., A. B. Hickman, F. Dyda, R. Ghirlando, D. R. Davies, and R. Craigie. Catalytic domain of human immunodeficiency virus type 1 integrase: identification of a soluble mutant by systematic replacement of hydrophobic residues. *Proc. Natl. Acad. Sci. USA* **92:**6057–6061 (1995).
37. Bujacz, G., M. Jaskolski, J. Alexandratos, A. Wlodawer, G. Merkel, R. A. Katz, and A. M. Skalka. The catalytic domain of avian sarcoma virus integrase: conformation of the active-site residues in the presence of divalent cations. *Structure* **4:**89–96 (1996).
38. Gulbis, J., and J. Everett, G. W. Metal binding characteristics of tetracycline derivatives in DMSO solution. *Tetrahedron* **32:**913–917 (1976).
39. Williamson, D. E., and J. Everett, G. W. A proton nuclear magnetic resonance study of the site of metal binding in tetracycline. *J. Am. Chem. Soc.* **97:**2397–2405 (1975).

Send reprint requests to: Dr. Yves Pommier, Laboratory of Molecular Pharmacology, Division of Basic Sciences, NCI/NIH, Bldg. 37, Room 5DO2, Bethesda, MD 20892. E-mail: pommier@nih.gov